LEDGF/p75 is Required for an Efficient DNA Damage Response

Victoria Liedtke
BTU: Brandenburgische Technische Universitat Cottbus-Senftenberg
Christian Schröder
BTU: Brandenburgische Technische Universitat Cottbus-Senftenberg
Dirk Roggenbuck
BTU: Brandenburgische Technische Universitat Cottbus-Senftenberg
Romano Weiss
BTU: Brandenburgische Technische Universitat Cottbus-Senftenberg
Ralf Stohwasser
BTU: Brandenburgische Technische Universitat Cottbus-Senftenberg
Peter Schierack
Brandenburgische Technische Universitat Cottbus-Senftenberg
Stefan Rödiger
Brandenburgische Technische Universitat Cottbus-Senftenberg
Lysann Schenk (Lysann.Schenk@b-tu.de)
Brandenburg University of Technology Cottbus-Senftenberg

Research

Keywords: LEDGF, CRISPR/Cas9, DNA damage signalling, γH2AX, ubiquitination

Posted Date: November 24th, 2020

DOI: https://doi.org/10.21203/rs.3.rs-111961/v1

Abstract

Background

Lens epithelium derived growth factor splice variant of 75 kDa (LEDGF/p75), is overexpressed in different solid cancers and cancer cell lines and various autoinflammatory diseases. Due to its ability to bind chromatin, it acts as a transcriptional co-activator and promotes anti-apoptotic signalling pathways that lead to increased tumour aggressiveness and resistance to chemotherapy. The role of LEDGF/p75 in DNA-damage repair (DDR) is still not completely elucidated particularly regarding the ubiquitin-dependent regulation and degradation of DDR signalling molecules.

Methods

Different LEDGF model cell lines were generated, a complete knock-out of LEDGF (KO) as well as the re-expression of LEDGF/p75 or LEDGF/p52 using CRISPR/Cas9 technology. Then, various assays were performed to determine their proliferation and migration capacity as well as their chemosensitivity. Moreover, DDR signalling pathways were investigated by western blot and immunofluorescence.

Results

LEDGF-deficient cells exhibited a decreased proliferation (d_t (WT) = 21 h, d_t (KO) = 26 h) , 60 % decreased migration, as well as an 30-50 % increased sensitivity towards the topoisomerase II inhibitor etoposide. Moreover, LEDGF depleted cells showed a significant reduction by 65 % in the recruitment of downstream DDR-related proteins like replication protein A 32 kDa subunit (RPA32) after exposure to etoposide. Re-expression of LEDGF/p75 rescued all knock-out effects, while re-expression of LEDGF/p52 had no effect.

Surprisingly, untreated LEDGF KO cells showed an increased amount of DNA fragmentation combined with an increased formation of γH2AX and Breast cancer type 1 susceptibility protein (BRCA1). In contrast, the protein levels of ubiquitin-conjugating enzyme UBC13 and nuclear proteasome activator PA28γ were substantially reduced upon LEDGF KO.

Conclusions

This study provides evidence that LEDGF is not only an important player in the DDR after chemotherapeutic treatments but is also involved in the maintenance of the general genome integrity. Moreover, this study provides for the first time an insight into the possible role of LEDGF in the ubiquitin-dependent regulation of DDR signalling molecules and highlights the involvement of LEDGF/p75 in homology-directed DNA repair.

Background

Dense fine speckled autoantigen of 70 kDa (DFS70) also known as lens epithelium derived growth factor (LEDGF), PSIP1 (PC4 and SFRS1 interacting protein 1) or transcriptional co-activator p75 is considered

an ubiquitous nuclear transcription co-activator (Basu *et al.*, 2015). It is linked to various diseases such as cancer, acquired immunodeficiency syndrome (AIDS) and diverse inflammatory conditions has been described (Debyser *et al.*, 2015; Leitz *et al.*, 2014) . LEDGF/p75 shows anti-apoptotic activity by promoting the repair of DNA double strand breaks (DSBs) *via* homology-directed repair pathway (HDR) (Daugaard *et al.*, 2007) and its overexpression in different cancer cell lines and solid tumours has been linked to tumour progression, aggressiveness and chemoresistance (Daniels *et al.*, 2005). In contrast, the shorter splice variant LEDGF/p52 has been proposed to play a pro-apoptotic role and also appears to be involved in RNA-splicing (Brown-Bryan *et al.*, 2008; Pradeepa *et al.*, 2012).

LEDGF/p75 is a multi-functional, chromatin-binding protein upregulated in different solid cancer and cancer cell lines (Basu *et al.*, 2015), promoting the activation of pathways involved in proliferation, cell survival and DNA repair (Basu *et al.*, 2012; Daugaard *et al.*, 2007; Ochs *et al.*, 2016). SUMOylation of LEDGF/p75 (Ishihara *et al.*, 2012) by sumo-specific protease-1 regulates its binding in promoter regions of stress-related proteins. This protects cells from stress-induced necrosis and enhances the activation of Akt/ERK signalling pathway, resulting in an increased tumour aggressiveness (Basu *et al.*, 2015; Bhargavan *et al.*, 2012).

Besides the upregulation in response to oxidative stress, the mechanism by which LEDGF/p75 protects cancer cells from stress-induced necrosis is not clarified. However, LEDGF/p75 can activate the expression of cancer-related genes e.g. vascular endothelial growth factor C (VEGF-C) as a transcriptional coactivator by protein-protein interaction (Basu *et al.*, 2012; Fatma *et al.*, 2001; Ríos-Colón *et al.*, 2017). It has been shown in prostate cancer cells that LEDGF/p75 facilitates chemotherapy resistance by counteracting caspase-independent apoptosis (Ríos-Colón *et al.*, 2017).

DNA damage response (DDR) is a finely tuned signalling network required to repair potentially lethal DNA DSBs and other DNA lesions. LEDGF/p75 interacting with this network supports rapid repair of DSBs. Thus, LEDGF/p75 recruits the histone acetyltransferase KAT5 to the chromatin which acetylates histone 4 (H4) at lysine K16 (Li and Wang, 2017). This acts as a switch between HDR and non-homologous end-joining (NHEJ). Upon H4 acetylation, the BRCA1-BARD1 complex can bind to DNA supporting HDR. Without H4 acetylation, BRCA1-BARD1 binding is inhibited by 53BP1 which in turn triggers NHEJ (Tang *et al.*, 2013).

Termination of DDR is accomplished by ubiquitination of key regulators such as γH2AX or BRCA1 (Gruosso *et al.*, 2016; Kim *et al.*, 2019). The LEDGF-dependent BRCA1-BARD-1 complex is a member of the E3-ubiquitin protein ligase family (Densham *et al.*, 2016). It is involved in ubiquitin-dependent regulation and signal termination of γH2AX (Mallery, 2002). Ubiquitination triggers degradation by the ubiquitin-proteasome system (UPS) and ubiquitin-independent proteasome pathway (UIPP) (Levy-Barda *et al.*, 2011).

We have created LEDGF knockout (KO), EGFP-LEDGF/p75 re-expressing (LEDGF/p75 o/e) and mEmarald_LEDGF/p52 re-expressing (LEDGF/p52 o/e) cells using CRISPR/Cas9 technology to analyze

the expression of various DDR proteins. Our work showed for the first time the participation of LEDGF/p75 in the ubiquitin-dependent regulation of DDR signalling molecules.

Materials And Methods

Antibodies

The following antibodies were used in this study: Anti-RPA32 (9H8), anti-N-PSIP1, anti-BRCA1 (G-9), UBC13 (F-10) (Santa Cruz Biotechnology, Texas, USA), anti-C-LEDGF/p75 (Bethyl-Laboratories, Texas, USA), anti-γH2AX (cell signalling), anti-PA28γ (K5.6), α-Mouse-IgG-Atto 488 N (Sigma Aldrich, Missouri, USA), α-rabbit-IgG-Atto 647 (Dianova, Hamburg, Germany) anti-mouse-IgG_K BP-HRP (Santa Cruz Biotechnology, Texas, USA), anti-rabbit HRP (Sigma Aldrich, Missouri, USA).

Cell lines and culture

Human epithelial type 2 (HEp-2) and human bone osteosarcoma epithelial cells (U2OS) wild type (WT) cells as well as LEDGF knockout (KO), EGFP-LEDGF/p75 re-expressing (LEDGF/p75) and mEmarald_LEDGF/p52 re-expressing (LEDGF/p52) cells were grown up to 80 % confluence in DMEM/Ham's F12 supplemented with 10 % FBS (Biowest, Nuaillé, France), 2 mM L-glutamine (Merck Millipore, Massachusetts, USA) and penicillin/streptomycin (Merck Millipore, Massachusetts, USA) in a humidified incubator at 37 °C and 5 % CO_2

Cloning

For the generation of LEDGF KO cells, sgRNA_DF70_E1 (AGATGAAAGGTTATCCCCAT, targeting exon 1 of *PSIP1* gene) was cloned into pSpCas9(BB)-2A-GFP (PX458; Addgene plasmid # 48138), kindly provided by Feng Zhang, Ph.D. (Ran *et al.*, 2013). Plasmids for EGFP-LEDGF/p75 overexpression (o/e were) created by cloning sgRNA_AAVS1 (CCAATCCTGTCCCTAG, targeting *AAVS1* locus) into pSpCas9(BB)-2A-GFP and gBlock HDR fragment (attB-sites, EGFP-LEDGF/p75 coding sequence, Supplement 4) into pAAVS1-P-CAG-DEST (Addgene plasmid #80490), kindly provided by Knut Woltjen, Ph.D. (Oceguera-Yanez, 2016). Plasmid for LEDGF/p52 o/e was created by cloning gBlock HDR fragment (attB-sites, mEmarald_LEDGF/p52 coding sequence, Supplement 5) into pAAVS1-P-CAG-DEST as described in the GATEWAY Cloning Technology Instruction Manual.

Generation of LEDGF modified cell clones

HEp-2 WT and U2OS WT cells were seeded in 6-well plates (TH. Geyer, Renningen, Germany), incubated for 24 h and subsequently transfected with px458_sgR_DFS70_E1 using Lipofectamine™ 3000 according to manufacturer's instructions (Thermo Fisher Scientific, Massachusetts, USA). For the EGFP-LEDGF/p75 o/e, WT and LEDGF KO cells were co-transfected with px458_sgRNA_AAVS1 and pAAVS1_CAG-EGFP-LEDGF/p75. Generation of mEmarald_LEDGF/p52 o/e cells was performed similar, but cells were co-transfected with px458_sgRNA_AAVS1 and pAAVS1_CAG-mEmarald_LEDGF/p52. Transfected cells were enriched by EGFP selection of biomarkers via FACS using S3e cell sorter (Bio-Rad).

Briefly, cells were resuspended in 1 x PBS supplemented with 0.5 % FBS, doublet cells were excluded by bivalent plotting of FSC and SSC, positively transfected cells were sorted by GFP expression. Per 10 cm^2 cell culture plate a total of $1x10^3$ cells were seeded. Outgrown fluorescent, single cell colonies were picked after 7-10 days.

Proliferation analysis

To determine cell proliferation, cells were seeded at a density of $5x10^3$ cells/well in a 96-well plate (Th.Geyer, Renningen, Germany) and Sulforhodamine B (SRB) assay was performed according to nature protocol (Vichai and Kirtikara, 2006).

Exposure to etoposide

Cells were seeded at $5x10^3$ cells/well into 96-well plates (Th.Geyer, Renningen, Germany) and incubated for 24 h. Subsequently, cells were exposed to different levels of etoposide (between 2.5-20 µM).

Digital image analysis and bioimage informatics

Analysis of cell viability was performed using a fully automatized multispectral fluorescence microscopy VideoScan platform (Rödiger *et al.*, 2012b; Willitzki *et al.*, 2013). Cells were stained with DAPI (2 µg/mL, Merck Millipore, Massachusetts, USA) in 1x PBS (Biowest, Nuaillé, France) and incubated 15 min at 37 °C, 5 % CO_2, following VideoScan analysis with exposure time of 0.5-1 s. Cell count per image was measured via Blob detection as implemented in scikit-image (blob_log; v.0.17.2) (SiMon, 2020) Images were further analysed using bioimage informatics by Python 3.7 script as described elsewhere (Schneider *et al.*, 2019, SilMon, 2020).

Cell morphology was analysed via calculation of the roundness and eccentricity of each cell. For that, firstly each cell with its corresponding nuclei was extracted as a set of points via thresholding (1.96 % of max. possible pixel intensity) and extraction of foreground pixels. Under segmented areas were detected via the overlap of multiple nuclei with one area. Each region containing multiple nuclei was segmented via a seeded flood fill approach. Thereby, the center of all corresponding nuclei were used as seed points for segmentation. Cell eccentricity was calculated via the second order area moments. Roundness R was estimated as the normalized ratio between area A and perimeter P of the cell by the equation $R = (4 * \pi * A) / P$.

The morphology of cells was separated into normal and fibroblast-like via **D**ensity-**B**ased **S**patial **C**lustering of **A**pplications with **N**oise (DBSCAN) clustering as implemented in the Python 3.7 package scikit-learn v. 0.23.1 (eps = 0.15, min_samples = 45).

Scratch assay

For measuring *in vitro* migration, $1x10^5$ cells/well were seeded in 48-well plates (Sarstedt, Nümbrecht, Germany) and incubated for 24 h. To stop proliferation, cells were treated with mitomycin C (10 µg/mL,

abcr GmbH, Karlsruhe, Germany) for 2 h, then washed and incubated for 22 h at 37 °C, 5 % CO_2. Circular scratch were created using 100 µL pipette tip and measured after 0 h and 24 h. Scratch area were analysed using ImageJ-macro MRI_would_healing_tool (http://dev.mri.cnrs.fr/projects/imagej-macros/wiki/Wound_Healing_Tool).

Immunofluorescence

Cells were seeded at 5 x 10^3 cells/well on 10-well slides (Hecht Assistant, Sondheim v. d. Rhön, Germany) and incubated for 24 h. For analysis, cells were fixed with 2 % formaldehyde for 15 min at RT and permeabilized with 0.3 % Triton X-100 (AppliChem, Darmstadt, Germany) while blocking with 5 % BSA/PBS. Primary antibody was added and incubated at RT for 1 h. Slides were washed with 1x PBS, then incubated with secondary antibody and DAPI (2.5 mg/mL, 1:500) for 1 h in the dark at RT. Fluorophore photostability was increased by coating slides with mounting medium (Roti®-Mount FluorCare, Carl Roth GmbH, Karlsruhe, Germany). Analysis was performed using a confocal laser scanning microscope LSM 800 (Zeiss, Oberkochen, Germany). Foci formation (250-500 nuclei/image) was analysed using NucDetect software (NucDetect 0.11.14, written in Python 3.7, available at https://pypi.org/project/NucDetect/).

Immunoblotting

Cells (1 x 10^6) were harvested and resuspended in 50 µL 2 x Lämmli-buffer and protein content was determined using Pierce™ BCA Protein Assay Kit (Thermo Fisher Scientific, Massachusetts, USA). Immunoblotting was performed using standard protocols (Ni *et al.*, 2017). Antibodies were diluted in 5 % milk powder or 5 % BSA (Carl Roth, Karlsruhe, Germany) in TBS/0.1 % Tween-20 (AppliChem, Darmstadt, Germany). The band intensity was quantified by ImageJ software (1.53c 26).

Pulsed field gel electrophoresis (PFGE)

Cells were seeded at 2x10^6 cells/10 cm dish and incubated for 24 h. Cells were treated as indicated, harvested, cell pellets were resuspended in 1 x PBS/peqGOLD agarose (VRW, Erlangen, Germany) (1:1) and used to cast inserts. Inserts were solidified at 4 °C until and then incubated in ESP buffer, (0.5 M EDTA (Carl Roth, Karlsruhe, Germany), 1 % (w/v) N-laurylsarcosine (Carl Roth, Karlsruhe, Germany) supplemented with 1.8 mg/mL proteinase K (≤ 30 mAnson U/mg, Carl Roth, Karlsruhe, Germany) at 56 °C for 18-20 h. Inserts were washed twice in 1 x TE buffer for 2 h at 4 °C, 10 rpm. Inserts were transferred to a 1.2 % peqGOLD agarose (VWR, Darmstadt, Germany) gel in 0.5 x TBE buffer (44.5 mM Tris-borate and 1 mM EDTA (pH 8.3)) and run at 6 V/cm, 5-50 s switch time for 22 h at 14 °C in PFGE chamber (Bio-Rad Genepath Electrophoresis Gel Cell, Bio-Rad, California, United States).

Statistical analysis

All data were statistically analysed with the statistical computing language R v. 3.6 (R: The R Project for Statistical Computing, 2020). The Kolmogorov-Smirnov test was used for testing of normal distribution.

To control the α error inflation, the Bonferroni correction is applied or the Tukey's HSD test is used to test the differences between the mean values of the sample for significance. P-values less than 0.05 were considered as significant. Experiments were conducted with at least three biological replicates. Data were further analysed using RKWard v. 0.7.1z+0.7.2+devel2 (Rödiger *et al*., 2012) for the R statistical computing environment. Dose-response curves were fitted (95 % confidence interval) with multiparametric functions (EXD3: Three-parameter exponential decay model; LL4: Four-parameter log-logistic model) from the drc package (Ritz *et al*., 2015). The optimal model was selected by using the AIC (Akaike information criterion) as criterion.

Results

CRISPR/Cas9–generated LEDGF cell models

For complete knockout of the LEDGF gene *PSIP1*, the sgRNA was designed within exon 1 of the *PSIP1* gene to target all splice variants (Fig. 1A). Therefore, HEp-2 WT and U2OS WT cells were transfected with non-viral px458_DFS70_E1 vector co-expressing EGFP as marker and Cas9 enzyme and enriched via EGFP-directed FACS sorting (Supplement 1A) following single cell out growth. The LEDGF KO HEp-2 clones were verified on protein and genomic level (Fig. 1E and Supplement 1C, D). Potential genomic off-target loci were checked by sequencing and exhibited all unmodified loci (Supplement 1E). Reconstitution of LEDGF in LEDGF KO realized by integration of either EGFP-LEDGF/p75 expression cassette (Fig. 1B) or mEmarald_LEDGF/p52 expression cassette at the human safe harbour locus (*AAVS1*) (Fig. 1E, F, Supplement 1B). EGFP-LEDGF/p75 and mEmarald_LEDGF/p52 incorporation and constitutive expression was confirmed by detecting the fluorescent LEDGF fusion protein (Fig. 1C). Both expressed splice variants showed the typical nuclear localisation. Additionally, C-terminal LEDGF antibody was used to detect the wildtype LEDGF and EGFP-LEDGF/p75 to show the typical dense fine speckled nuclear staining pattern (Fig. 1D). Note, mEmarald_LEDGF/p52 cannot be detected with this antibody as p52 is missing the C-terminus.

Depletion of LEDGF decreases cellular migration

LEDGF has been previously shown to affect cell migration. Therefore, cell migration of HEp-2 and U2OS cells was checked. Indeed, the migratory capacity was significantly reduced upon LEDGF knockout in HEp-2 and U2OS cells (Fig. 2C). LEDGF/p52 re-expression failed to restore the migration capacity of the HEp-2 WT (Fig. 2A, C). In contrast, LEDGF/p75 re-expression reversed the inhibiting effect and caused even higher cell migration with increased LEDGF expression (Fig. 2C) than characteristic for the unmodified WT cells. Additionally, EGFP-LEDGF/p75 o/e cells showed a changed morphology towards an elongated, fibroblast-like phenotype in combination (Fig. 2D) with an increased expression of the cytoskeleton subunit α-tubulin (Fig. 2B). Morphological analysis revealed that LEDGF/p75 o/e cells exhibited a significantly increased eccentricity and a significantly decreased round shape by 50 % ($p < 0.05$, Fig. 2D). However, LEDGF KO cells showed a reduced expression of α-tubulin but no change in morphology (Fig. 2 B).

LEDGF depletion sensitizes cancer cells towards etoposide

LEDGF KO cells showed a significant decrease in cell proliferation in comparison to the WT cells while cell cycle progression was not affected (Fig. 3A and Supplement 3A, B). The re-expression of LEDGF/p75 completely rescued the proliferation rate implicating that the p75 splice variant is the most relevant for cell growth.

Upon etoposide exposure, LEDGF KO cells showed a significantly reduced cell survival (Fig. 3B). ED_{50} determinations confirmed that LEDGF plays a critical role in chemo-sensitivity towards etoposide (Fig. 3C). We were able to compensate the reduced survival of LEDGF KO cells (ED_{50} = 0.123 ± 0.01) by re-expressing LEDGF (EGFP-LEDGF/p75 o/e, ED_{50} = 0.4 ± 0.04), which resulted in an etoposide resistance equal to unmodified WT-cells (ED_{50} = 0.317 ± 0.03) (Fig. 3B, C).

LEDGF depletion impairs DNA damage response via homology-directed repair

LEDGF has been previously implicated to play a crucial role in HDR-mediated damage response involving CtIP-BRCA1-RPA32 signalling. RPA32 foci formation was used as a surrogate to detect active HR.

Here, LEDGF knockout in HEp-2 cells caused a significant increase sensitivity towards etoposide (Fig. 3B-C). This was accompanied by a massive DNA fragmentation (Fig. 4B) and phosphorylation of H2AX (γH2AX, Fig. 4A) indicating etoposide-induced DSBs, which was similar to wildtype HEp-2 cells. However, the phosphorylation of RPA32 was almost completely abolished in LEDGF KO cells while wildtype cells showed an elevated phosphorylation level (Fig. 4A). This was also reflected by significantly reduced RPA32 foci formation (Fig. 4C-D) after etoposide treatment in LEDGF KO cells indicating an inhibition of CtIP-BRCA1-mediated homology-directed repair. The re-expression of LEDGF/p75 was able to rescue the RPA32 foci formation (Fig. 4C-D).

LEDGF depletion results in dysfunctional DNA damage response

Interestingly, γH2AX was increased already without DSB-inducing agents in LEDGF KO cells (Fig. 4A). Additionally, pulse-field electrophoresis revealed an increased amount of fragmented DNA in untreated LEDGF KO cells (Fig. 4B). Surprisingly, LEDGF KO cells exhibited not only a significantly high number of persistent γH2AX foci (Fig. 5C, D and supplement 3C) but also a significantly increased foci formation of the DNA damage response molecule BRCA1 (Fig. 5A, B and supplement 3B). Both elevated foci formations were reversed by re-expression of EGFP-LEDGF/p75 (Fig. 5A-D and supplement 3B-C).

Despite the high “basal” γH2AX foci in LEDGF KO, indicating permanent DNA damage, the cells were able to be maintained over 20-30 passages without dying even though at significantly slower growth rate (Fig. 3A). Therefore, we were interested whether the sustained γH2AX foci are related to a dysregulated degradation of the histone. It has been previously stated that ubiquitination plays an important role in the regulation of DNA damage response signaling. For the γH2AX molecule, K63-linked ubiquitination by UBC13 is important in order to activate BRCA1-A complex which coordinates the release of γH2AX which

is subsequently degraded by the proteasome (Fig. 5G). However, this happens downstream of LEDGF-induced CtIP-BRCA1-RPA32 DNA damage signalling.

Here, we show for the first time that LEDGF depletion significantly reduced the protein expression levels of UBC13 as well as PA28γ also known as REGγ (Fig. 5E in Hep-2 and 5F in U2OS cells) which was reversed by LEDGF/p75 re-expression but not LEDGF/p52. This indicates a predominant role of LEDGF/p75 in the regulation of UBC13 and PA28γ which might affect not only γH2AX but also BRCA1 degradation.

Discussion

LEDGF/p75 has been reported to be overexpressed in different solid tumours and cancer cell lines (Bhargavan *et al.*, 2012; Daugaard *et al.*, 2007). Particularly, it is involved in cancer progression by controlling the expression of genes regulating cell cycle, cell proliferation and survival (Singh *et al.*, 2017). Furthermore, LEDGF/p75 is supposed to enhance HDR by promoting CtIP-BRCA1-dependent DNA end-resection after DNA DSB and influences the recruitment of DNA-damage response-related downstream proteins such as RPA32 (Daugaard *et al.*, 2012). Instead of siRNA knockdown with potential residual LEDGF expression, we generated complete *PSIP1* knockout using CRISPR/Cas9 technology. We show for the first time that complete LEDGF depletion has an essential influence on DDR signalling.

To avoid off-target effects due to plasmid integration and constitutive active Cas9 expression, LEDGF knockout generation was pursued using an EGFP reporter to enrich transient Cas9 and sgRNA expressing cells. Thus, effects detectable for EGFP-selected LEDGF KO clones should be based on LEDGF knockout, making the results more reliable. Potential off-target effects due to the sgRNA (Zhang *et al.*, 2015) were checked by sequencing (supplement 1E). Additionally, different LEDGF KO clones were tested for their uniform behaviour using a proliferation assay (supplement 2A). Moreover, LEDGF recovery experiments showed that the effects induced by LEDGF depletion could be rescued by EGFP-LEDGF/p75 re-expression indicating a specific knockout.

Increased LEDGF/p75 expression in prostate cancer (Mediavilla-Varela *et al.*, 2009), breast cancer (Daugaard *et al.*, 2007) or colon cancer (Basu *et al.*, 2015) was linked with an aggressive tumour phenotype. Furthermore, upregulation of LEDGF in prostate and breast cancer cell lines has been shown to play a role in proliferation, migration and chemoresistance (Ríos-Colón *et al.*, 2017; Singh *et al.*, 2017). In this presented study, proliferation and migration analysis of LEDGF depleted cells (Fig. 2-3) showed a significant reduction in cell growth and decreased migration ability, supporting LEDGF to be involved in pro-survival pathways as previously described (Ríos-Colón *et al.*, 2017). This is further underlined by the LEDGF/p75 o/e model in our study where increased expression resulted in enhanced migratory abilities. Moreover, these cells showed a change in morphology to a fibroblast-like phenotype which was accompanied with an increased expression of α-tubulin. Up to now, only acetylation of α-tubulin has been connected to cancer cell migration and invasion (Boggs *et al.*, 2015; Lee *et al.*, 2018). However, increased class III ß-tubulin has been associated with a more aggressive tumour phenotype (Lebok *et al.*, 2016).

LEDGF depletion sensitizes cells towards caspase-dependent cell death on etoposide exposure (Ríos-Colón *et al.*, 2017). In this work, characterization of LEDGF KO clones confirmed a direct correlation of LEDGF depletion with a reduced proliferation and an increased sensitivity towards topoisomerase II inhibition by etoposide.

As previously shown elsewhere (Brown-Bryan *et al.*, 2008; Daugaard *et al.*, 2012; Huang *et al.*, 2007), the re-expression of the shorter splice variant LEDGF/p52 has no enhancing effect on the cell proliferation, migration or chemosensitivity.

Daugaard *et al.* demonstrated LEDGF as an important factor in DNA repair via HDR. After induction of a DNA DSB, the ensuing cellular damage response leads either to NHEJ or HDR. In contrast to NHEJ, HDR is only active in late S-and G2-phase (Lin *et al.*, 2014). Moreover, LEDGF KO cells exhibit a decreased survival and elevated DNA fragmentation upon etoposide exposure which might indicate a deficiency to repair DNA DSBs by HDR. Therefore, RPA32 foci formation was investigated and indeed, in LEDGF knockout clones, less RPA32 was recruited to the DNA damage sites in comparison to the wild type cells. In fact, LEDGF/p75 is known to bind to methylated histones, supporting the binding of C-terminal binding protein (CtBP) interacting protein (CtIP) and assists DNA damage recognition by MRN complex (Daugaard *et al.*, 2012). Subsequently, this activates three main damage response-related protein kinases: ATM, ATR and DNA PKs. RPA32, also active during replication, is activated by ATM and ATR, resulting in phosphorylated RPA32 foci formation, necessary for the recruitment of downstream DNA repair proteins (Liu *et al.*, 2012).

The reduced amount of RPA32 foci in LEDGF-KO clones is consistent with the results of Daugaard et al (2012) which implies that LEDGF is necessary for the recruitment of HDR-related DNA repair proteins and is required for an efficient DNA repair. Moreover, the elevated γH2AX foci formation upon LEDGF KO suggests that LEDGF plays a role in the maintenance of genome stability. In fact, SETD2 depletion resulted also in an increased γH2AX foci formation (Kanu *et al.*, 2015) SETD2 trimethylates histone-3 lysine-36 (H3K36me3) at sites of active transcription and the histone code reader LEDGF/p75 binds to it (Li and Wang, 2017). Furthermore, persistent γH2AX are an indicator for “oncogenic stress”, DNA damage driving genomic instability and malignant conversion (Bartkova *et al.*, 2005). Chromosomal instability and gene mutations in cancer cells are well described (reviewed in Vargas-Rondón *et al.*, 2017) and are often caused by increased DNA DSBs with dysregulated DNA repair mechanisms. Since LEDGF/p75 is involved in the HDR-mediated DNA repair, its depletion might leave more DNA DSBs unrepaired. In cancer cells, spontaneous DNA damage foci formation (increase in γH2AX foci formation) caused by self-inflicting or endogenous DNA DSBs are often observed. We were able to show that in LEDGF KO cells those endogenous DNA DSBs are significantly increased. Controversially, LEDGF KO cells could be cultured (with decreased proliferation) and are not prone to go directly into apoptosis which suggests that LEDGF interacts with further signalling pathways.

Finally, increased phosphorylation of H2AX can be also caused in response to cell cycle progression during G2/M phase entry (An *et al.*, 2010). Therefore, a potential cell cycle arrest in LEDGF KO cells was

investigated, especially because LEDGF knockdown has been previously shown to induce cell cycle arrest in S/G2 phase and increased apoptosis in prostate cancer cells (Bhargavan *et al.*, 2012). Nonetheless, in our study, cell cycle profiles of WT and LEDGF-depleted cells were similar without any sign of cell arrest in LEDGF KO cells (supplement 2B).

An efficient and coordinated degradation of signalling molecules is necessary for an efficient DDR which is accompanied by a vast amount of proteasome-independent K63-linked ubiquitin modifications of the signalling molecules. At the end of the signal transduction, many DDR-involved molecules e.g. γH2AX are degraded by the proteasome (Gruosso et al., 2016; Krum et al., 2010; Ramadan and Meerang, 2011). Additionally, it has been shown that the knockout of the nuclear proteasome activator PA28γ led to persistent γH2AX foci, even after signal termination (Levy-Barda *et al.*, 2011). These persistent γH2AX foci interfere with new DNA damage signals, which lead to an overall reduced DDR and thus to genetically unstable cells. As demonstrated for PA28γ knockout cells, LEDGF depletion also resulted in a decreased PA28γ protein level. This might indicate that the sustained γH2AX foci and BRCA1 foci are also a result of diminished degradation of these molecules. Moreover, the proteasome recycles ubiquitin by degrading proteins which is required indirectly for the ubiquitin signalling in DDR as it supplies the DNA repair ligases e.g. UBC13 with ubiquitin (Stone and Morris, 2014). UBC13 expression was also abrogated in the LEDGF KO cells.

Conclusion

In summary, the present study underlined the crucial role of LEDGF/p75 in homology-directed repair after DNA damage through chemotherapeutics but also its involvement in cellular processes such as migration and proliferation. Moreover, this study indicates for the first time that LEDGF/p75 potentially participates in the regulation of damage response-signalling by modulating the expression of ubiquitin-conjugating enzymes such as UBC13 and nuclear proteasome activator which subsequently leads to an altered degradation of DDR signalling molecules.

Abbreviations

53BP1 – p53-binding protein 1

BRCA1- breast cancer type 1 susceptibility protein

CRISPR – clustered regulatory interspaced short palindromic repeats

CtIP – CtBP (C-terminal binding protein) interacting protein

DAPI – 4',6-Diamidin-2-phenylindol

DBSCAN – Density-Based Spatial Clustering of Applications with Noise

DDR – DNA damage repair

DSBs – double strand breaks

ED50 – effective dose for 50% of the population

FACS – Fluorescence Activated Cell Sorting

GFP / EGFP – Green Fluorescent Protein / Enhanced Green Fluorescent Protein

HDR – homology-directed repair

KO – knockout

LEDGF- lens epithelium derived growth factor

LEDGF/p75 - lens epithelium derived; growth factor, splice variant of 75 kDa

LEDGF/p52 - lens epithelium derived growth factor, splice variant of 52 kDa

NHEJ – non-homologous end-joining

PA28γ – PSM3E - Proteasome activator complex subunit 3

PSIP1 – PC4 And SFRS1 Interacting Protein 1

RPA32 – Replication protein A 32 kDa subunit

UBC13 – Ubiquitin-conjugating enzyme E2 13

VEGF-C – Vascular Endothelial Growth Factor C

WT – wildtype

γH2AX – phosphorylated Histone H2AX

Declarations

Ethics approval and consent to participate

Not applicable.

Consent for publication

Not applicable.

Availability of data and material

Not applicable.

Competing interests

The authors declare that they have no conflict of interest.

Funding

This work was supported by the "Gesundheitscampus Brandenburg - Konsequenzen der altersassoziierten Zell - und Organfunktionen" [GeCa: H228-05/002/008, 2017-2019] initiative of the Brandenburgian Ministry of Science, Research and Culture (MWFK, Germany), PRAEMED.BIO – Präzisionsmedizin durch biomarkerbasierte Diagnostik of the Federal Ministry of Education and Research (03WKDB2C, BMBF, Germany) and the Friedrich-Naumann Foundation for Freedom.

Authors contribution

LS, VL and CS designed the experiments and provided the theoretical background for the study. VL conducted all experiments, prepared figures and illustrations together with LS and wrote the manuscript together with LS, SR and DR. RW designed the software for the evaluation of the proliferation and killing assays and performed DB scan analysis for the cell morphology determination. SR designed the software for the ED_{50} calculation and assisted with the statistical analysis. RS provided the theory and material to the proteasome work in the study. Funding acquisition by SR, PS and LS. All authors read and approved the final manuscript.

Acknowledgements

We would like to thank Madeleine Ruhe, Franziska Dinter and Julia Engelmann for their support during the conduction of experiments.

References

An, J., Huang, Y.-C., Xu, Q.-Z., Zhou, L.-J., Shang, Z.-F., Huang, B., Wang, Y., Liu, X.-D., Wu, D.-C., Zhou, P.-K., 2010. DNA-PKcs plays a dominant role in the regulation of H2AX phosphorylation in response to DNA damage and cell cycle progression. BMC Mol. Biol. 11, 18. https://doi.org/10.1186/1471-2199-11-18

SilMon. (2020, November 13). SilMon/Cell-Morphology-Notebook: v. 1.1 (Version v1.1). Zenodo. http://doi.org/10.5281/zenodo.4271745

Bartkova, J., Hořejší, Z., Koed, K., Krämer, A., Tort, F., Zieger, K., Guldberg, P., Sehested, M., Nesland, J.M., Lukas, C., Ørntoft, T., Lukas, J., Bartek, J., 2005. DNA damage response as a candidate anti-cancer barrier in early human tumorigenesis. Nature 434, 864–870. https://doi.org/10.1038/nature03482

Basu, A., Rojas, H., Banerjee, H., Cabrera, I.B., Perez, K.Y., De León, M., Casiano, C.A., 2012. Expression of the Stress Response Oncoprotein LEDGF/p75 in Human Cancer: A Study of 21 Tumor Types. PLoS ONE 7, e30132. https://doi.org/10.1371/journal.pone.0030132

Basu, A., Woods-Burnham, L., Ortiz, G., Rios-Colon, L., Figueroa, J., Albesa, R., Andrade, L.E., Mahler, M., Casiano, C.A., 2015. Specificity of antinuclear autoantibodies recognizing the dense fine speckled nuclear pattern: Preferential targeting of DFS70/LEDGFp75 over its interacting partner MeCP2. Clin. Immunol. 161, 241–250. https://doi.org/10.1016/j.clim.2015.07.014

Bhargavan, B., Fatma, N., Chhunchha, B., Singh, V., Kubo, E., Singh, D.P., 2012. LEDGF gene silencing impairs the tumorigenicity of prostate cancer DU145 cells by abating the expression of Hsp27 and activation of the Akt/ERK signaling pathway. Cell Death Dis. 3, e316. https://doi.org/10.1038/cddis.2012.57

Boggs, A.E., Vitolo, M.I., Whipple, R.A., Charpentier, M.S., Goloubeva, O.G., Ioffe, O.B., Tuttle, K.C., Slovic, J., Lu, Y., Mills, G.B., Martin, S.S., 2015. α-Tubulin Acetylation Elevated in Metastatic and Basal-like Breast Cancer Cells Promotes Microtentacle Formation, Adhesion, and Invasive Migration. Cancer Res. 75, 203–215. https://doi.org/10.1158/0008-5472.CAN-13-3563

Brown-Bryan, T.A., Leoh, L.S., Ganapathy, V., Pacheco, F.J., Mediavilla-Varela, M., Filippova, M., Linkhart, T.A., Gijsbers, R., Debyser, Z., Casiano, C.A., 2008. Alternative Splicing and Caspase-Mediated Cleavage Generate Antagonistic Variants of the Stress Oncoprotein LEDGF/p75. Mol. Cancer Res. 6, 1293–1307. https://doi.org/10.1158/1541-7786.MCR-08-0125

Daugaard, M., Baude, A., Fugger, K., Povlsen, L.K., Beck, H., Sørensen, C.S., Petersen, N.H.T., Sorensen, P.H.B., Lukas, C., Bartek, J., Lukas, J., Rohde, M., Jäättelä, M., 2012. LEDGF (p75) promotes DNA-end resection and homologous recombination. Nat. Struct. Mol. Biol. 19, 803–810. https://doi.org/10.1038/nsmb.2314

Daugaard, M., Kirkegaard-Sorensen, T., Ostenfeld, M.S., Aaboe, M., Hoyer-Hansen, M., Orntoft, T.F., Rohde, M., Jaattela, M., 2007. Lens Epithelium-Derived Growth Factor Is an Hsp70-2 Regulated Guardian of Lysosomal Stability in Human Cancer. Cancer Res. 67, 2559–2567. https://doi.org/10.1158/0008-5472.CAN-06-4121

Debyser, Z., Christ, F., De Rijck, J., Gijsbers, R., 2015. Host factors for retroviral integration site selection. Trends Biochem. Sci. 40, 108–116. https://doi.org/10.1016/j.tibs.2014.12.001

Densham, R.M., Garvin, A.J., Stone, H.R., Strachan, J., Baldock, R.A., Daza-Martin, M., Fletcher, A., Blair-Reid, S., Beesley, J., Johal, B., Pearl, L.H., Neely, R., Keep, N.H., Watts, F.Z., Morris, J.R., 2016. Human BRCA1–BARD1 ubiquitin ligase activity counteracts chromatin barriers to DNA resection. Nat. Struct. Mol. Biol. 23, 647–655. https://doi.org/10.1038/nsmb.3236

Fatma, N., Singh, D.P., Shinohara, T., Chylack, L.T., 2001. Transcriptional Regulation of the Antioxidant Protein 2 Gene, a Thiol-specific Antioxidant, by Lens Epithelium-derived Growth Factor to Protect Cells from Oxidative Stress. J. Biol. Chem. 276, 48899–48907. https://doi.org/10.1074/jbc.M100733200

Gruosso, T., Mieulet, V., Cardon, M., Bourachot, B., Kieffer, Y., Devun, F., Dubois, T., Dutreix, M., Vincent-Salomon, A., Miller, K.M., Mechta-Grigoriou, F., 2016. Chronic oxidative stress promotes H2 AX protein degradation and enhances chemosensitivity in breast cancer patients. EMBO Mol. Med. 8, 527–549. https://doi.org/10.15252/emmm.201505891

Huang, T., Myklebust, L.M., Kjarland, E., Gjertsen, B., Pendino, F., Bruserud, Ø., Døskeland, S., Lillehaug, J.R., 2007. LEDGF/p75 has increased expression in blasts from chemotherapy-resistant human acute myelogenic leukemia patients and protects leukemia cells from apoptosis in vitro. Mol. Cancer 6, 31. https://doi.org/10.1186/1476-4598-6-31

Ishihara, K., Fatma, N., Bhargavan, B., Chhunchha, B., Kubo, E., Dey, S., Takamura, Y., Kumar, A., Singh, D.P., 2012. Lens epithelium-derived growth factor deSumoylation by Sumo-specific protease-1 regulates its transcriptional activation of small heat shock protein and the cellular response: Senp-1 regulates LEDGF transcriptional activity. FEBS J. 279, 3048–3070. https://doi.org/10.1111/j.1742-4658.2012.08686.x

Kanu, N., Grönroos, E., Martinez, P., Burrell, R.A., Yi Goh, X., Bartkova, J., Maya-Mendoza, A., Mistrík, M., Rowan, A.J., Patel, H., Rabinowitz, A., East, P., Wilson, G., Santos, C.R., McGranahan, N., Gulati, S., Gerlinger, M., Birkbak, N.J., Joshi, T., Alexandrov, L.B., Stratton, M.R., Powles, T., Matthews, N., Bates, P.A., Stewart, A., Szallasi, Z., Larkin, J., Bartek, J., Swanton, C., 2015. SETD2 loss-of-function promotes renal cancer branched evolution through replication stress and impaired DNA repair. Oncogene 34, 5699–5708. https://doi.org/10.1038/onc.2015.24

Kim, S., Jin, H., Seo, H.-R., Lee, H.J., Lee, Y.-S., 2019. Regulating BRCA1 protein stability by cathepsin S-mediated ubiquitin degradation. Cell Death Differ. 26, 812–825. https://doi.org/10.1038/s41418-018-0153-0

Krum, S.A., Dalugdugan, E. de la R., Miranda-Carboni, G.A., Lane, T.F., 2010. BRCA1 Forms a Functional Complex with γ -H2AX as a Late Response to Genotoxic Stress. J. Nucleic Acids 2010, 1–9. https://doi.org/10.4061/2010/801594

Lebok, P., Öztürk, M., Heilenkötter, U., Jaenicke, F., Müller, V., Paluchowski, P., Geist, S., Wilke, C., Burandt, E., Lebeau, A., Wilczak, W., Krech, T., Simon, R., Sauter, G., Quaas, A., 2016. High levels of class III β-tubulin expression are associated with aggressive tumor features in breast cancer. Oncol. Lett. 11, 1987–1994. https://doi.org/10.3892/ol.2016.4206

Lee, C.-C., Cheng, Y.-C., Chang, C.-Y., Lin, C.-M., Chang, J.-Y., 2018. Alpha-tubulin acetyltransferase/MEC-17 regulates cancer cell migration and invasion through epithelial–mesenchymal transition suppression and cell polarity disruption. Sci. Rep. 8. https://doi.org/10.1038/s41598-018-35392-6

Leitz, J., Reuschenbach, M., Lohrey, C., Honegger, A., Accardi, R., Tommasino, M., Llano, M., von Knebel Doeberitz, M., Hoppe-Seyler, K., Hoppe-Seyler, F., 2014. Oncogenic Human Papillomaviruses Activate the Tumor-Associated Lens Epithelial-Derived Growth Factor (LEDGF) Gene. PLoS Pathog. 10, e1003957. https://doi.org/10.1371/journal.ppat.1003957

Levy-Barda, A., Lerentha, Y., Davis, A.J., Chung, Y.M., Essers, J., Shao, Z., Vliet, N. van, Che, D.J., Hu, M.C.-T., Kanaar, R., Ziv, Y., Shiloh, Y., 2011. Involvement of the nuclear proteasome activator PA28γ in the cellular response to DNA doublestrand break. Cell Cycle. https://doi.org/10.4161/ cc.10.24.18642

Li, L., Wang, Y., 2017. Cross-talk between the H3K36me3 and H4K16ac histone epigenetic marks in DNA double-strand break repair. J. Biol. Chem. 292, 11951–11959. https://doi.org/10.1074/jbc.M117.788224

Lin, S., Staahl, B.T., Alla, R.K., Doudna, J.A., 2014. Enhanced homology-directed human genome engineering by controlled timing of CRISPR/Cas9 delivery. eLife 3. https://doi.org/10.7554/eLife.04766

Liu, S., Opiyo, S.O., Manthey, K., Glanzer, J.G., Ashley, A.K., Amerin, C., Troksa, K., Shrivastav, M., Nickoloff, J.A., Oakley, G.G., 2012. Distinct roles for DNA-PK, ATM and ATR in RPA phosphorylation and checkpoint activation in response to replication stress. Nucleic Acids Res. 40, 10780–10794. https://doi.org/10.1093/nar/gks849

Mallery, D.L., 2002. Activation of the E3 ligase function of the BRCA1/BARD1 complex by polyubiquitin chains. EMBO J. 21, 6755–6762. https://doi.org/10.1093/emboj/cdf691

Mediavilla-Varela, M., Pacheco, F.J., Almaguel, F., Perez, J., Sahakian, E., Daniels, T.R., Leoh, L., Padilla, A., Wall, N.R., Lilly, M.B., De Leon, M., Casiano, C.A., 2009. Docetaxel-induced prostate cancer cell death involves concomitant activation of caspase and lysosomal pathways and is attenuated by LEDGF/p75. Mol. Cancer 8, 68. https://doi.org/10.1186/1476-4598-8-68

Oceguera-Yanez, F., 2016. Engineering the AAVS1 locus for consistent and scalable transgene expression in human iPSCs and their differentiated derivatives 13.

Ochs, R.L., Mahler, M., Basu, A., Rios-Colon, L., Sanchez, T.W., Andrade, L.E., Fritzler, M.J., Casiano, C.A., 2016. The significance of autoantibodies to DFS70/LEDGFp75 in health and disease: integrating basic science with clinical understanding. Clin. Exp. Med. 16, 273–293.

Pradeepa, M.M., Sutherland, H.G., Ule, J., Grimes, G.R., Bickmore, W.A., 2012. Psip1/Ledgf p52 Binds Methylated Histone H3K36 and Splicing Factors and Contributes to the Regulation of Alternative Splicing. PLoS Genet. 8, e1002717. https://doi.org/10.1371/journal.pgen.1002717

R: The R Project for Statistical Computing [WWW Document], n.d. URL https://www.r-project.org/ (accessed 6.3.20).

Ramadan, K., Meerang, M., 2011. Degradation-linked ubiquitin signal and proteasome are integral components of DNA double strand break repair: New perspectives for anti-cancer therapy. FEBS Lett. 585, 2868–2875. https://doi.org/10.1016/j.febslet.2011.04.046

Ran, F.A., Hsu, P.D., Wright, J., Agarwala, V., Scott, D.A., Zhang, F., 2013. Genome engineering using the CRISPR-Cas9 system. Nat. Protoc. 8, 2281–2308. https://doi.org/10.1038/nprot.2013.143

Ríos-Colón, L., Ross, C.K.C.-D., Basu, A., Elix, C., Alicea-Polanco, I., Sanchez, T.W., Radhakrishnan, V., Chen, C.-S., Casiano, C.A., 2017. Targeting the stress oncoprotein LEDGF/p75 to sensitize chemoresistant prostate cancer cells to taxanes. Oncotarget 8. https://doi.org/10.18632/oncotarget.15323

Ritz, C., Baty, F., Streibig, J.C., Gerhard, D., 2015. Dose-Response Analysis Using R. PLOS ONE 10, e0146021. https://doi.org/10.1371/journal.pone.0146021

Rödiger, S., Friedrichsmeier, T., Kapat, P., Michalke, M., 2012a. RKWard: a comprehensive graphical user interface and integrated development environment for statistical analysis with R. J. Stat. Softw. 49, 1–34. https://doi.org/10.18637/jss.v049.i09

Rödiger, S., Schierack, P., Böhm, A., Nitschke, J., Berger, I., Frömmel, U., Schmidt, C., Ruhland, M., Schimke, I., Roggenbuck, D., Lehmann, W., Schröder, C., 2012b. A Highly Versatile Microscope Imaging Technology Platform for the Multiplex Real-Time Detection of Biomolecules and Autoimmune Antibodies, in: Seitz, H., Schumacher, S. (Eds.), Molecular Diagnostics, Advances in Biochemical Engineering/Biotechnology. Springer Berlin Heidelberg, Berlin, Heidelberg, pp. 35–74. https://doi.org/10.1007/10_2011_132

Schneider, J., Weiss, R., Ruhe, M., Jung, T., Roggenbuck, D., Stohwasser, R., Schierack, P., Rödiger, S., 2019. Open source bioimage informatics tools for the analysis of DNA damage and associated biomarkers. J. Lab. Precis. Med. 21–21. https://doi.org/10.21037/jlpm.2019.04.05

SilMon. (2020, November 13). SilMon/Cell-Morphology-Notebook: v. 1.1 (Version v1.1). Zenodo. http://doi.org/10.5281/zenodo.4271745

Singh, D.K., Gholamalamdari, O., Jadaliha, M., Ling Li, X., Lin, Y.-C., Zhang, Y., Guang, S., Hashemikhabir, S., Tiwari, S., Zhu, Y.J., Khan, A., Thomas, A., Chakraborty, A., Macias, V., Balla, A.K., Bhargava, R., Janga, S.C., Ma, J., Prasanth, S.G., Lal, A., Prasanth, K.V., 2017. PSIP1/p75 promotes tumorigenicity in breast cancer cells by promoting the transcription of cell cycle genes. Carcinogenesis 38, 966–975. https://doi.org/10.1093/carcin/bgx062

Stone, H.R., Morris, J.R., 2014. DNA damage emergency: cellular garbage disposal to the rescue? Oncogene 33, 805–813. https://doi.org/10.1038/onc.2013.60

Tang, J., Cho, N.W., Cui, G., Manion, E.M., Shanbhag, N.M., Botuyan, M.V., Mer, G., Greenberg, R.A., 2013. Acetylation limits 53BP1 association with damaged chromatin to promote homologous recombination. Nat. Struct. Mol. Biol. 20, 317–325. https://doi.org/10.1038/nsmb.2499

Vargas-Rondón, N., Villegas, V., Rondón-Lagos, M., 2017. The Role of Chromosomal Instability in Cancer and Therapeutic Responses. Cancers 10, 4. https://doi.org/10.3390/cancers10010004

Vichai, V., Kirtikara, K., 2006. Sulforhodamine B colorimetric assay for cytotoxicity screening. Nat. Protoc. 1, 1112–1116. https://doi.org/10.1038/nprot.2006.179

Willitzki, A., Lorenz, S., Hiemann, R., Guttek, K., Goihl, A., Hartig, R., Conrad, K., Feist, E., Sack, U., Schierack, P., Heiserich, L., Eberle, C., Peters, V., Roggenbuck, D., Reinhold, D., 2013. Fully automated analysis of chemically induced γH2AX foci in human peripheral blood mononuclear cells by indirect immunofluorescence: Fully Automated γH2AX Foci Analysis in PBMCs. Cytometry A 83, 1017–1026. https://doi.org/10.1002/cyto.a.22350

Figures

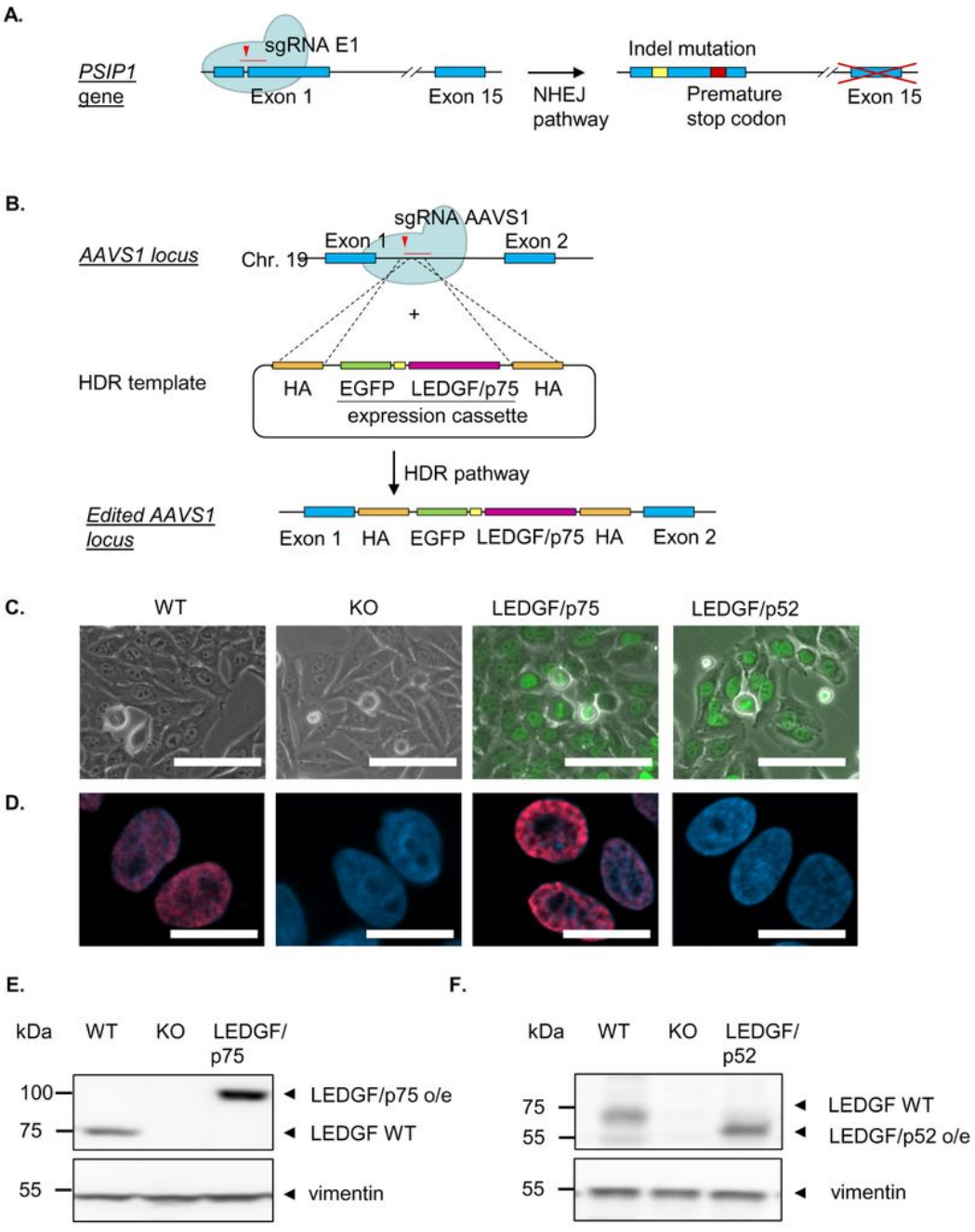

Figure 1

Verification of CRISPR/Cas9-mediated LEDGF knockout and LEDGF re-expression in HEp-2 cells. A. Specific sgRNA for Exon 1 of LEDGF-coding gene PSIP1 was designed to knockout LEDGF. B. LEDGF/p75 and LEDGF/p52 re-expressing cells were created by introducing a DNA DSB at genomic safe-harbour locus (AAVS1) using an AAVS1-specific sgRNA. After the induction of a DSB, homology-directed repair (HDR) mediates the integration of the donor template containing the EGFP-LEDGF/p75 or a

mEmarald_LEDGF/p52 expression cassette at the AAVS1 locus. Generated LEDGF knockout and re-expressing cells were verified by C. fluorescence analysis with an excitation wavelength of 488 nm (scale bar = 100 µm), D. indirect immunofluorescence (IF). Anti C-LEDGF antibody appear red due to conjugation to α-rabbit-IgG-Atto 647 secondary antibody, nuclei appear blue due to DAPI incorporation (scale bar = 20 µm) E. Immunoblot using antibodies against C-terminal LEDGF and vimentin as loading control. F. Immunoblot with antibodies against N-terminal LEDGF and vimentin as loading control.

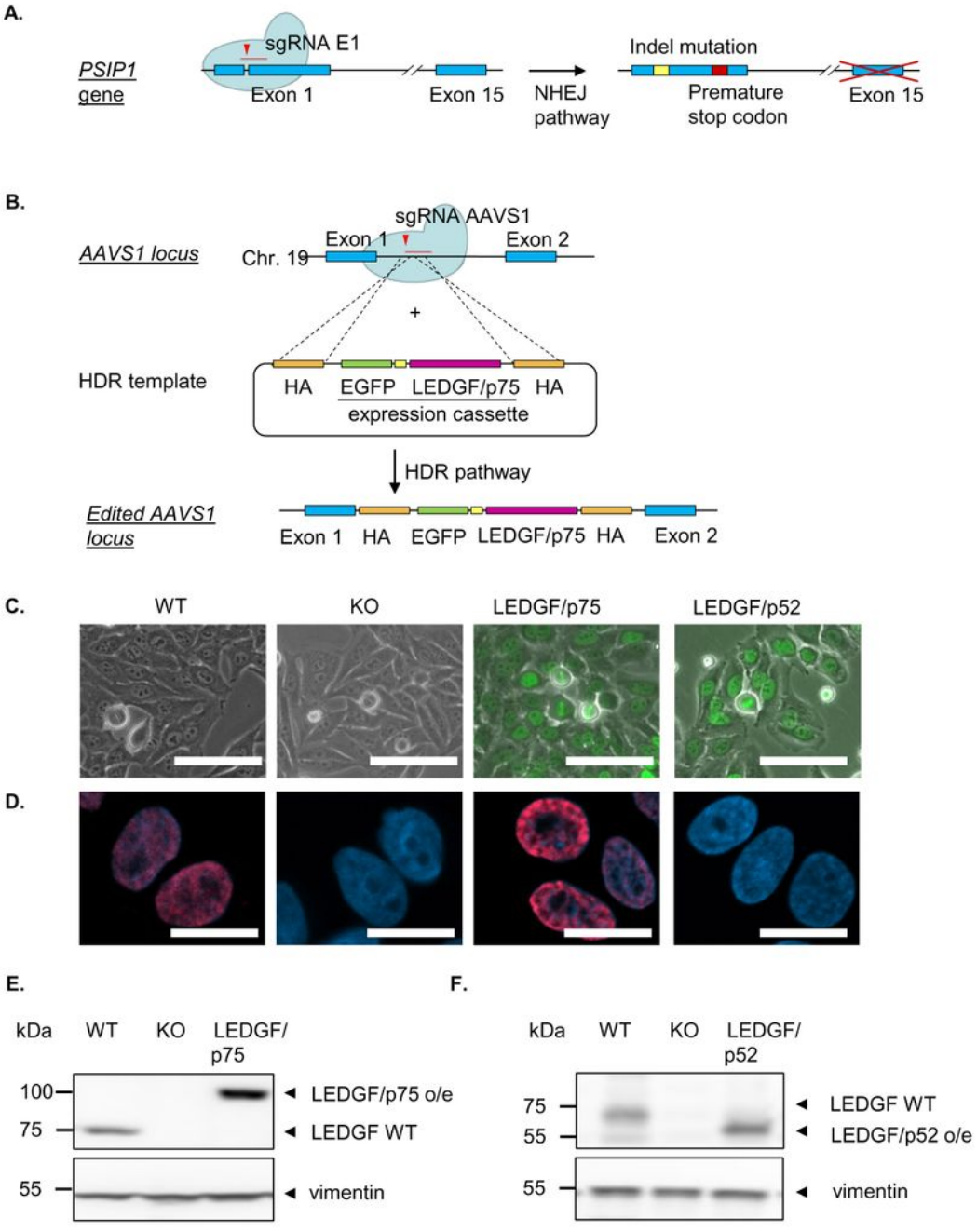

Figure 1

Verification of CRISPR/Cas9-mediated LEDGF knockout and LEDGF re-expression in HEp-2 cells. A. Specific sgRNA for Exon 1 of LEDGF-coding gene PSIP1 was designed to knockout LEDGF. B. LEDGF/p75 and LEDGF/p52 re-expressing cells were created by introducing a DNA DSB at genomic safe-harbour locus (AAVS1) using an AAVS1-specific sgRNA. After the induction of a DSB, homology-directed repair (HDR) mediates the integration of the donor template containing the EGFP-LEDGF/p75 or a mEmarald_LEDGF/p52 expression cassette at the AAVS1 locus. Generated LEDGF knockout and re-expressing cells were verified by C. fluorescence analysis with an excitation wavelength of 488 nm (scale bar = 100 µm), D. indirect immunofluorescence (IF). Anti C-LEDGF antibody appear red due to conjugation to α-rabbit-IgG-Atto 647 secondary antibody, nuclei appear blue due to DAPI incorporation (scale bar = 20 µm) E. Immunoblot using antibodies against C-terminal LEDGF and vimentin as loading control. F. Immunoblot with antibodies against N-terminal LEDGF and vimentin as loading control.

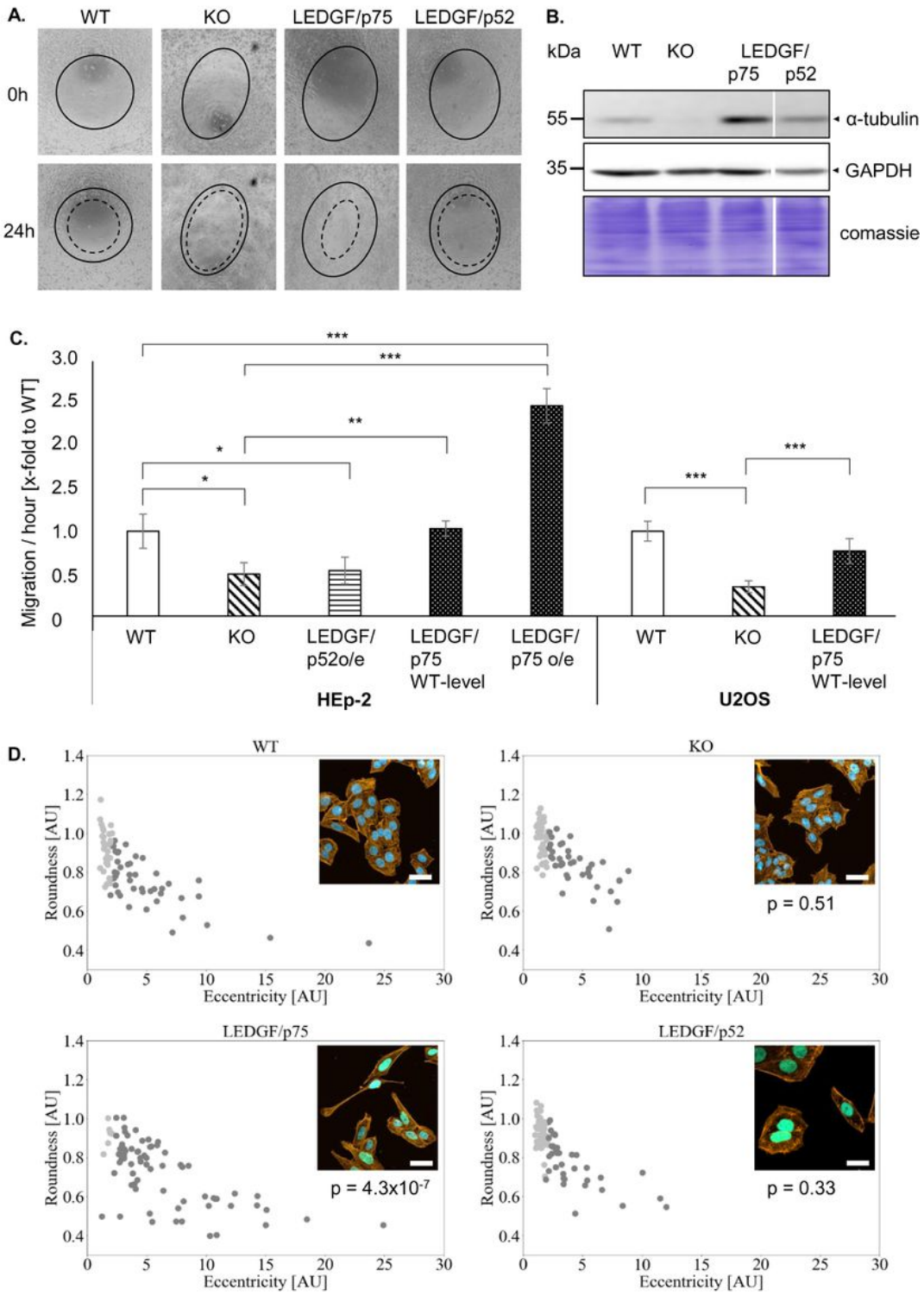

Figure 2

LEDGF influences cell migration and morphology. A. Representative phase contrast image of HEp-2 WT, LEDGF K.O., LEDGF/p75 and LEDGF/p52 overexpressing cells, 0 h (black line) and 24 h (dashed line) after creating a circular scratch in a cell monolayer. Prior to scratch, cells were incubated in 10 µg/mL mitomycin C prior to inhibiting cell proliferation. B. Immunoblot shows the level of α-tubulin in untreated cells. As loading control, gel was stained with Coomassie brilliant-blue to visualize total protein amount

(10µg/lane) and GAPDH antibody was used. C. The wound healing capacity of the indicated HEp-2 and U2OS cell clones were analysed using ImageJ plugin MRI wound-healing tool after 24 h of the scratch induction and plotted as area/hour. D. Representative confocal images of HEp-2 WT, LEDGF KO, LEDGF/p75 and LEDGF/p52 overexpressing cells were taken after incubation with Phalloidin-AlexaFluor555 (yellow). Chromatin appears blue due to DAPI incorporation, nuclei of LEDGF/p75 overexpressing cells appear green due to EGFP-tag of LEDGF/p75, scale bar = 20 µm. The images were used to perform a DBSCAN clustering correlating cell roundness and eccentricity in HEp-2 WT, LEDGF K.O., LEDGF/p75 and LEDGF/p52 overexpressing cells (n = 672, whereby only 75 cells are shown per condition). Cells with fibroblast-like morphology are shown in dark grey and cells with roundish morphology in light grey.

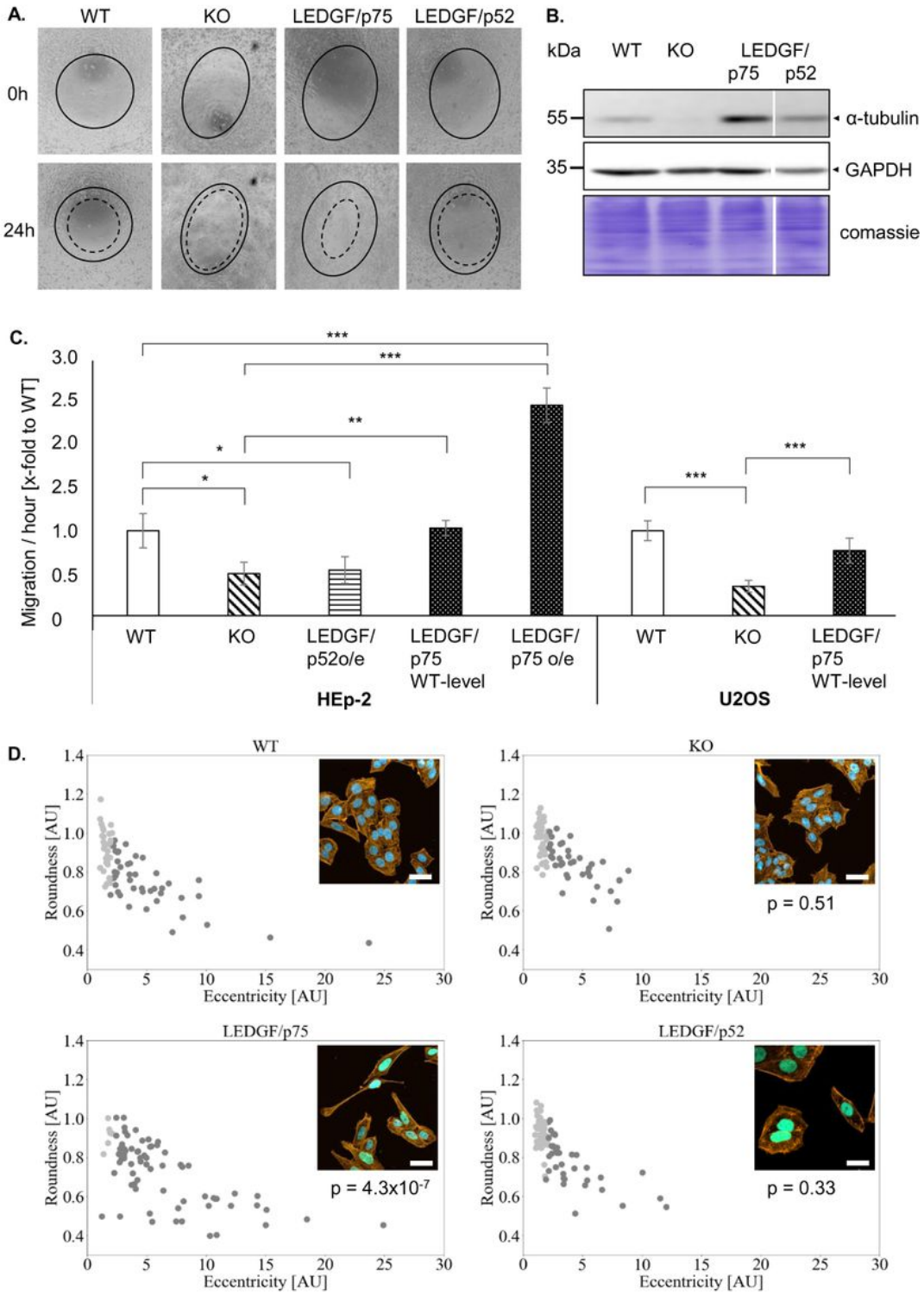

Figure 2

LEDGF influences cell migration and morphology. A. Representative phase contrast image of HEp-2 WT, LEDGF K.O., LEDGF/p75 and LEDGF/p52 overexpressing cells, 0 h (black line) and 24 h (dashed line) after creating a circular scratch in a cell monolayer. Prior to scratch, cells were incubated in 10 µg/mL mitomycin C prior to inhibiting cell proliferation. B. Immunoblot shows the level of α-tubulin in untreated cells. As loading control, gel was stained with Coomassie brilliant-blue to visualize total protein amount

(10µg/lane) and GAPDH antibody was used. C. The wound healing capacity of the indicated HEp-2 and U2OS cell clones were analysed using ImageJ plugin MRI wound-healing tool after 24 h of the scratch induction and plotted as area/hour. D. Representative confocal images of HEp-2 WT, LEDGF KO, LEDGF/p75 and LEDGF/p52 overexpressing cells were taken after incubation with Phalloidin-AlexaFluor555 (yellow). Chromatin appears blue due to DAPI incorporation, nuclei of LEDGF/p75 overexpressing cells appear green due to EGFP-tag of LEDGF/p75, scale bar = 20 µm. The images were used to perform a DBSCAN clustering correlating cell roundness and eccentricity in HEp-2 WT, LEDGF K.O., LEDGF/p75 and LEDGF/p52 overexpressing cells (n = 672, whereby only 75 cells are shown per condition). Cells with fibroblast-like morphology are shown in dark grey and cells with roundish morphology in light grey.

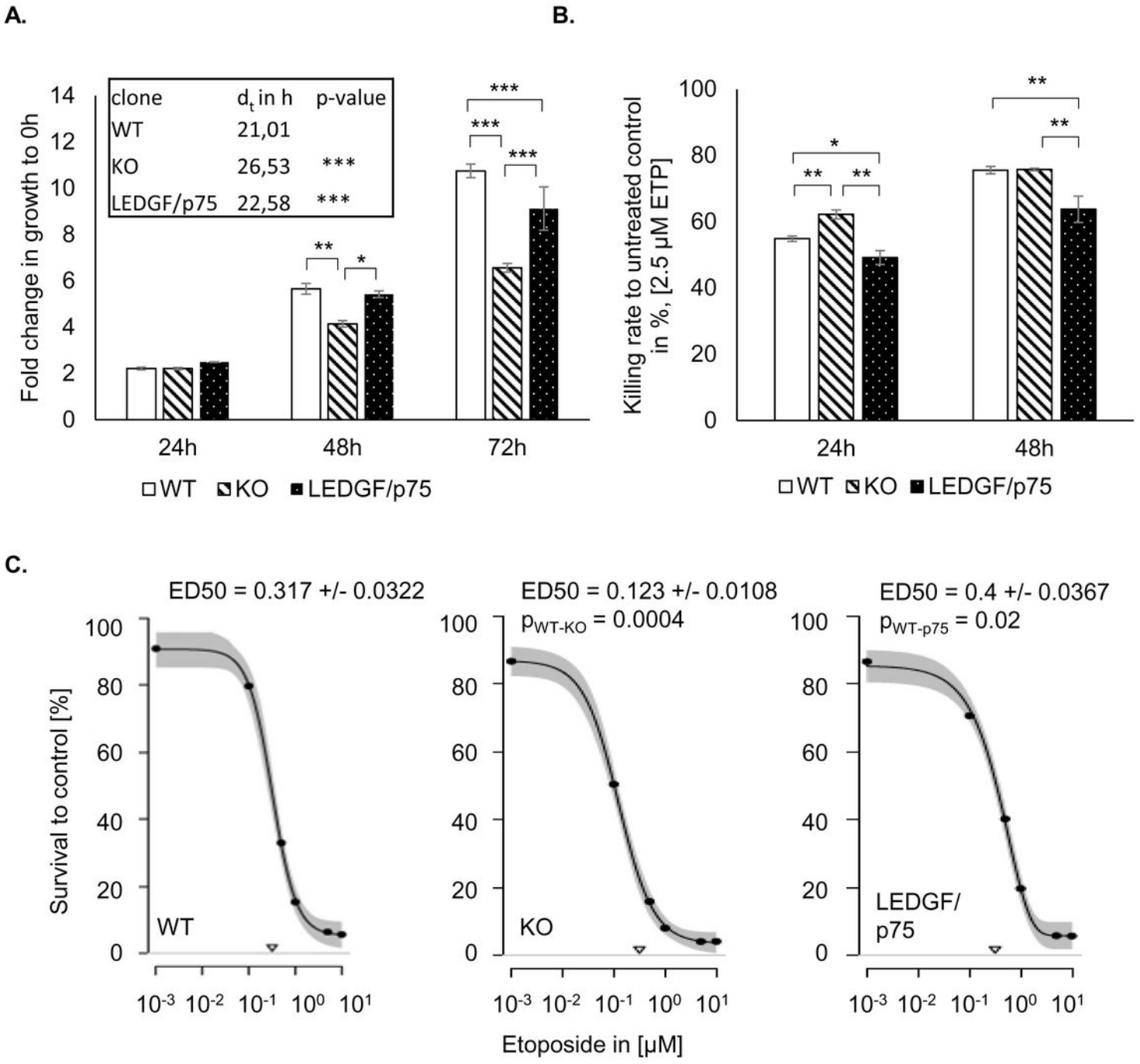

Figure 3

LEDGF affects cell proliferation and chemo-resistance. A. Proliferation of non-treated HEp-2 WT, LEDGF KO and LEDGF/p75 re-expressing cells were determined for 0 h, 24 h, 48 h (pWT-KO = 0.006, pKO-p75 = 0.015, pp75-WT = 0.705), and 72 h (pWT-KO = 3x10-6, pKO-p75 = 7x10-5, pp75-WT = 0.0008) by SRB assay. Doubling time (dt) was determined for HEp-2 WT, LEDGF KO and LEDGF/p75 re-expressing cell lines (pWT-KO = 3.4x10-5, pp75-KO = 2.6x10-4). B. After 24 h growth, indicated cell lines were treated with

1.25 µM etoposide for 24 h (pWT-KO = 0.010, pKO-p75 = 0.0004, pp75-WT = 0.022) and 48 h (pWT-KO = 0.044, pKO-p75 = 0.0002, pp75-WT = 0.0021) and the survival rate was determined in comparison to the untreated control. C. Determination of ED50 value of HEp-2 WT, LEDGF KO and LEDGF/p75 o/e cells after 48 h etoposide treatment, followed by 3 days of recovery. Dose-response curves were fitted (95 % confidence interval) with multiparametric functions (EXD3: Three-parameter exponential decay model; LL4: Four-parameter log-logistic model, pWT-KO = 0.0004, pWT-p75 = 0.02).

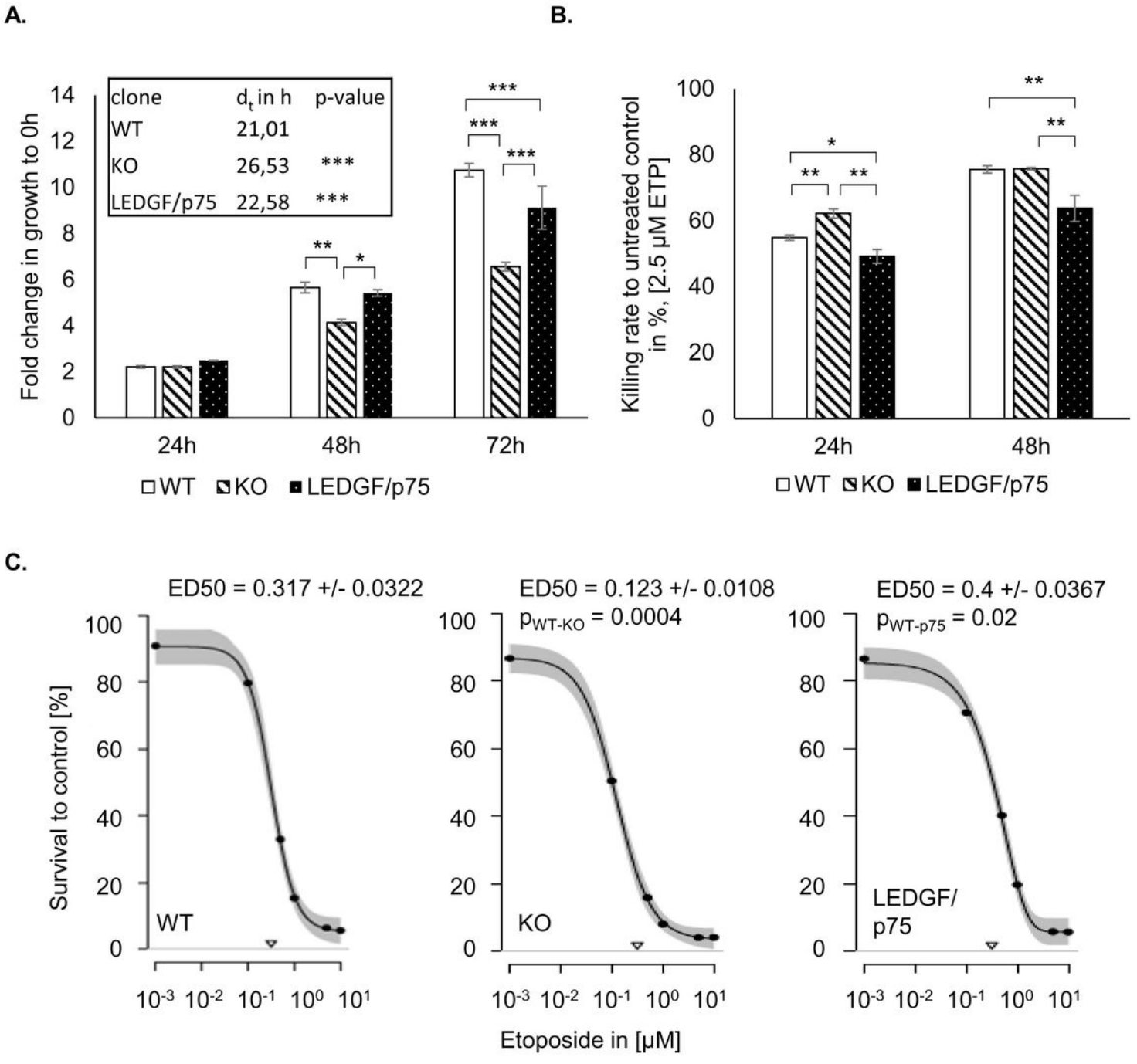

Figure 3

LEDGF affects cell proliferation and chemo-resistance. A. Proliferation of non-treated HEp-2 WT, LEDGF KO and LEDGF/p75 re-expressing cells were determined for 0 h, 24 h, 48 h (pWT-KO = 0.006, pKO-p75 = 0.015, pp75-WT = 0.705), and 72 h (pWT-KO = 3x10-6, pKO-p75 = 7x10-5, pp75-WT = 0.0008) by SRB assay. Doubling time (dt) was determined for HEp-2 WT, LEDGF KO and LEDGF/p75 re-expressing cell lines (pWT-KO = 3.4x10-5, pp75-KO = 2.6x10-4). B. After 24 h growth, indicated cell lines were treated with 1.25 µM etoposide for 24 h (pWT-KO = 0.010, pKO-p75 = 0.0004, pp75-WT = 0.022) and 48 h (pWT-KO = 0.044, pKO-p75 = 0.0002, pp75-WT = 0.0021) and the survival rate was determined in comparison to the untreated control. C. Determination of ED50 value of HEp-2 WT, LEDGF KO and LEDGF/p75 o/e cells after 48 h etoposide treatment, followed by 3 days of recovery. Dose-response curves were fitted (95 % confidence interval) with multiparametric functions (EXD3: Three-parameter exponential decay model; LL4: Four-parameter log-logistic model, pWT-KO = 0.0004, pWT-p75 = 0.02).

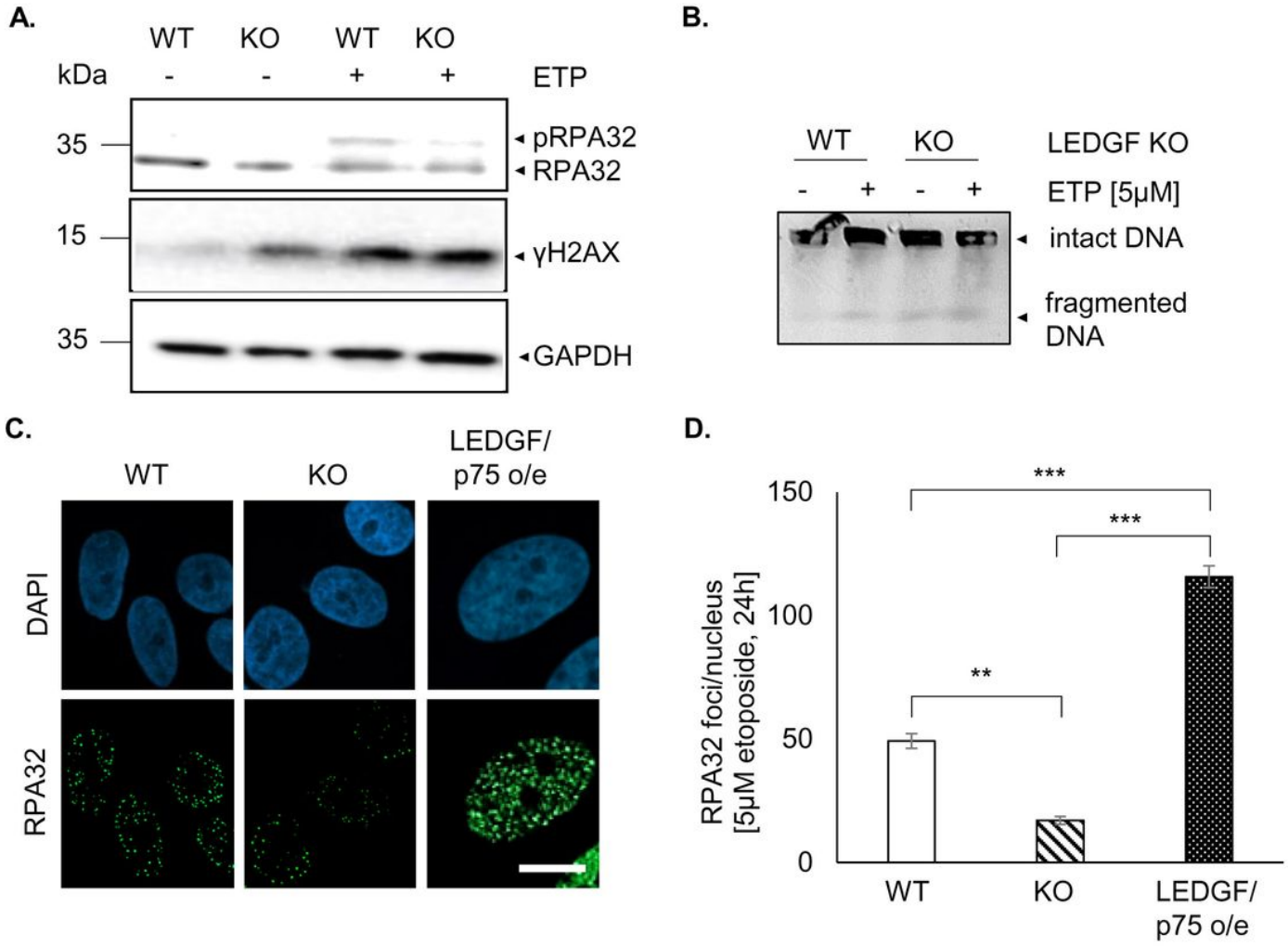

Figure 4

LEDGF necessary for CtIP-BRCA1-mediated homology-directed repair. A. Immunoblots show levels of pRPA32, RPA32, γH2AX and GAPDH in untreated cells and cells after treatment with 5 µM etoposide for 6

h. B. Pulsed field gel electrophoresis (PFGE) with 5x105 cells/insert of HEp-2 WT and LEDGF KO cells. Cells were either not treated (“-“) or treated with 5 µM ETP for 6 h (“+“). C. Representative images of RPA32 foci are shown in indicated cells treated with 5 µM etoposide for 16 h. Cells were fixed with 2 % formaldehyde and incubated anti-RPA32 (Santa Cruz Biotechnology, green). Chromatin appears blue due to DAPI incorporation. Scale bar: 10 µm. D. Analysis of RPA32 foci (at least 100 foci were counted) was performed using NucDetect software, n = 3, * p < 0.05, ** p < 0.01, *** p < 0.001.

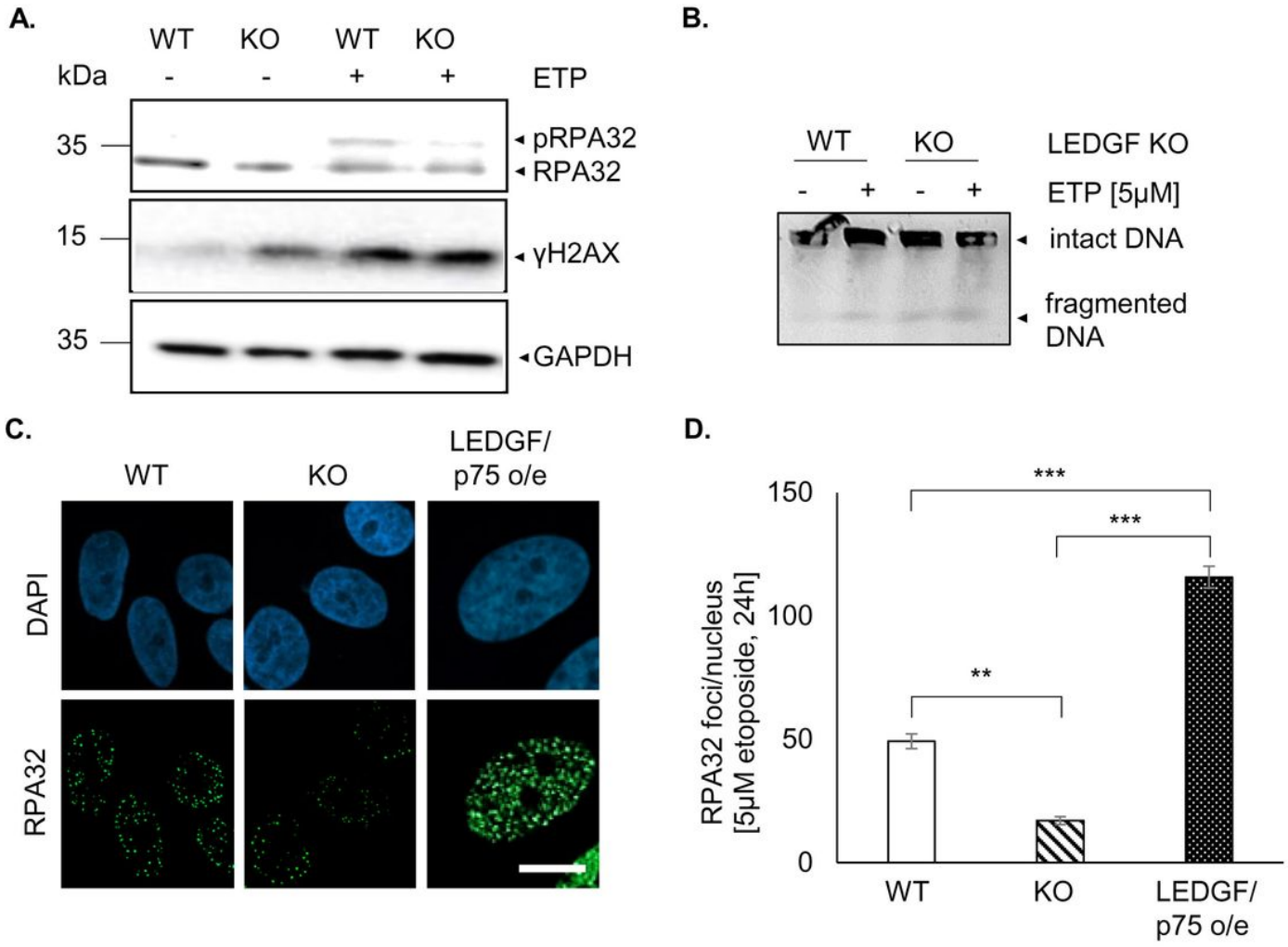

Figure 4

LEDGF necessary for CtIP-BRCA1-mediated homology-directed repair. A. Immunoblots show levels of pRPA32, RPA32, γH2AX and GAPDH in untreated cells and cells after treatment with 5 µM etoposide for 6 h. B. Pulsed field gel electrophoresis (PFGE) with 5x105 cells/insert of HEp-2 WT and LEDGF KO cells. Cells were either not treated (“-“) or treated with 5 µM ETP for 6 h (“+“). C. Representative images of RPA32 foci are shown in indicated cells treated with 5 µM etoposide for 16 h. Cells were fixed with 2 % formaldehyde and incubated anti-RPA32 (Santa Cruz Biotechnology, green). Chromatin appears blue due

to DAPI incorporation. Scale bar: 10 µm. D. Analysis of RPA32 foci (at least 100 foci were counted) was performed using NucDetect software, n = 3, * p < 0.05, ** p < 0.01, *** p < 0.001.

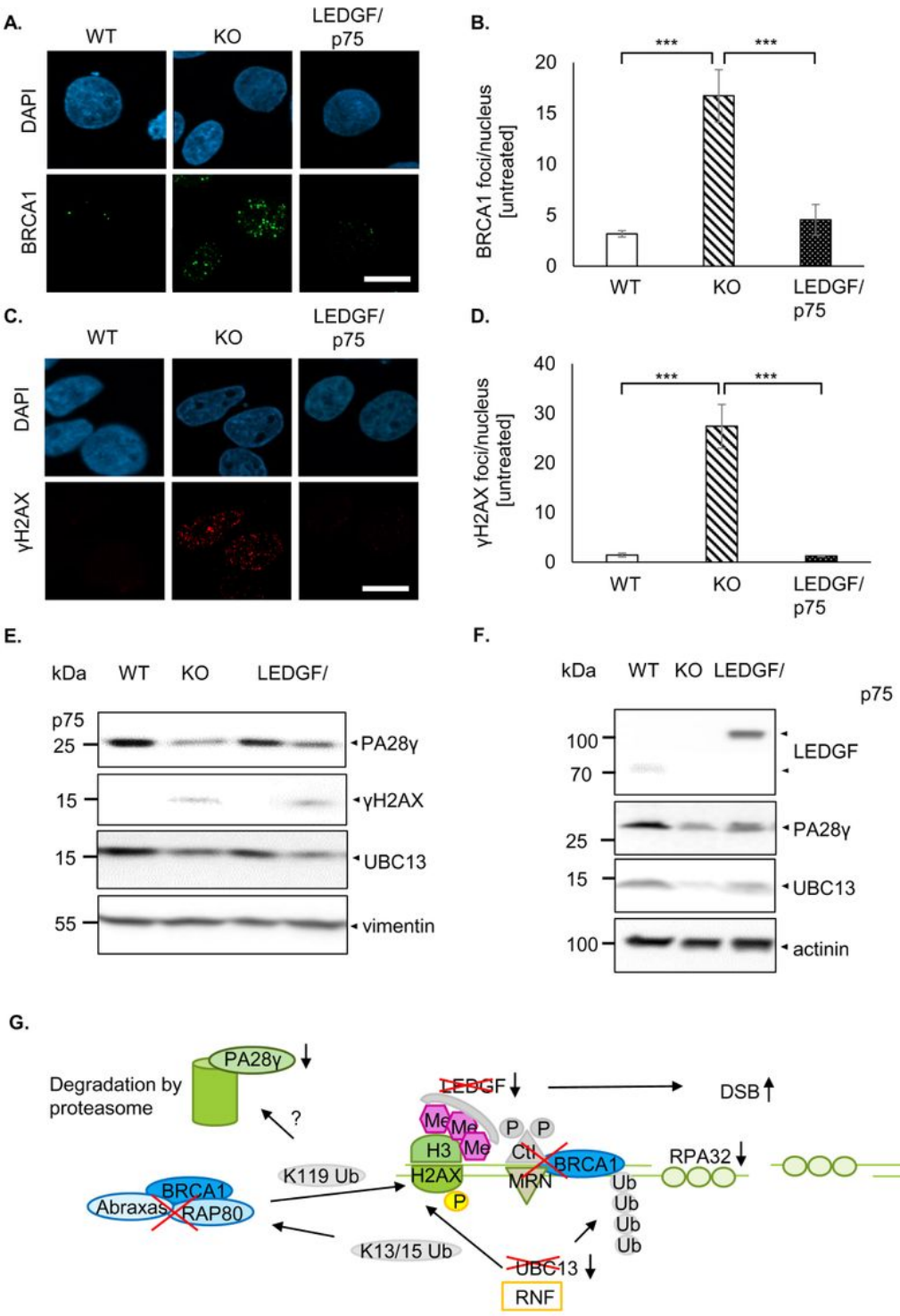

Figure 5

LEDGF depletion causes dysregulation of DNA damage response. A.+C. Representative confocal images of BRCA1 foci (A.) and γH2AX foci (C.) of untreated HEp-2 WT, LEDGF KO and LEDGF/p75 re-expressing cells are shown after fixation with 2 % formaldehyde and incubation with anti-γH2AX or anti-BRCA1.

Chromatin appears blue due to DAPI incorporation, BRCA1 (green) and γH2AX (red). Scale bar: 10 µm. B.+D. Analysis of BRCA1 foci (pWT-KO = 0.0005, pKO-p75 = 0.0008, pWT-p75 = 0.8100) (B.) and γH2AX foci (pWT-KO = 10-7, pKO-p75 = 10-7, pWT-p75 = 0.9934) (D.) in HEp-2 WT, LEDGF KO and LEDGF/p75 re-expressing cells using NucDetect software, n=3. * $p < 0.05$, ** $p < 0.01$, *** $p < 0.00$. E. Untreated HEp-2 cell lines were harvested after 48h and protein extracts were analysed by immunoblotting using antibodies against PA28γ, γH2AX, UBC13 and vimentin as loading control. F. According to A, untreated U2OS cell lines were analysed by immunoblotting. Vimentin was used as loading control. G. Scheme of the HDR-mediated DDR signalling after DSB. Initially, LEDGF recruits CtIP to the DNA damage site which forms a complex with MRN and BRCA1 thereby activating RPA32 and later Rad51 for the DNA end resection. Thus, UBC13 is activated to add K63-linked ubiquitin to lysine residues (K13/15) of γH2AX molecule, which in turn activates BRCA1-A complex (containing also Rap80 and Abraxas) which coordinates the release of γH2AX (ubiquitination at K119) from the chromatin leading to the subsequent degradation by the proteasome. The red crosses indicate the dysregulation of the pathway upon LEDGF KO.

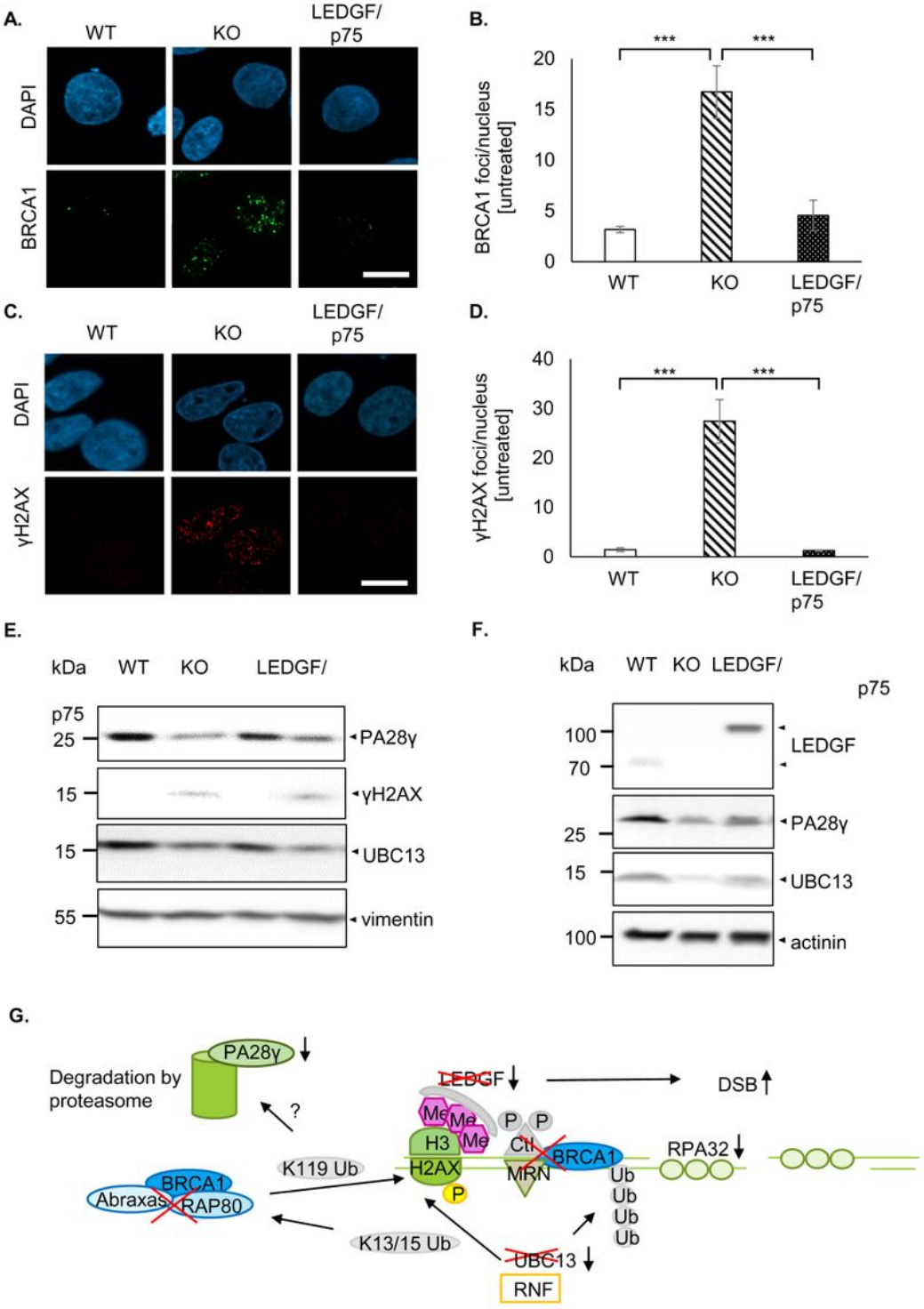

Figure 5

LEDGF depletion causes dysregulation of DNA damage response. A.+C. Representative confocal images of BRCA1 foci (A.) and γH2AX foci (C.) of untreated HEp-2 WT, LEDGF KO and LEDGF/p75 re-expressing cells are shown after fixation with 2 % formaldehyde and incubation with anti-γH2AX or anti-BRCA1. Chromatin appears blue due to DAPI incorporation, BRCA1 (green) and γH2AX (red). Scale bar: 10 µm. B.+D. Analysis of BRCA1 foci (pWT-KO = 0.0005, pKO-p75 = 0.0008, pWT-p75 = 0.8100) (B.) and γH2AX

foci (pWT-KO = 10-7, pKO-p75 = 10-7, pWT-p75 = 0.9934) (D.) in HEp-2 WT, LEDGF KO and LEDGF/p75 re-expressing cells using NucDetect software, n=3. * p < 0.05, ** p < 0.01, *** p < 0.00. E. Untreated HEp-2 cell lines were harvested after 48h and protein extracts were analysed by immunoblotting using antibodies against PA28γ, γH2AX, UBC13 and vimentin as loading control. F. According to A, untreated U2OS cell lines were analysed by immunoblotting. Vimentin was used as loading control. G. Scheme of the HDR-mediated DDR signalling after DSB. Initially, LEDGF recruits CtIP to the DNA damage site which forms a complex with MRN and BRCA1 thereby activating RPA32 and later Rad51 for the DNA end resection. Thus, UBC13 is activated to add K63-linked ubiquitin to lysine residues (K13/15) of γH2AX molecule, which in turn activates BRCA1-A complex (containing also Rap80 and Abraxas) which coordinates the release of γH2AX (ubiquitination at K119) from the chromatin leading to the subsequent degradation by the proteasome. The red crosses indicate the dysregulation of the pathway upon LEDGF KO.

Supplementary Files

This is a list of supplementary files associated with this preprint. Click to download.

- 201115sup.1.pdf
- 201115sup.1.pdf
- 201115sup.2.pdf
- 201115sup.2.pdf
- 201115sup.3.pdf
- 201115sup.3.pdf
- 201115sup.4.pdf
- 201115sup.4.pdf
- 201115sup.5.pdf
- 201115sup.5.pdf
- 201115sup.6.pdf
- 201115sup.6.pdf